18th Brazilian Congress of Thermal Sciences and Engineering
November 16-20, 2020 (Online)

# ENC-2020-0294
# THERMAL AND HYDRODYNAMIC BEHAVIOR OF HFE7100 CONVECTIVE BOILING IN A MICROCHANNEL-BASED HEAT SINK

**João Vitor Zago**[1]
zagojoavitor@gmail.com
**Victor Hugo Monghini**[1]
monghini.vh@gmail.com
**Reinaldo Rodrigues de Souza**[1]
reisartre@gmail.com
**Elaine Maria Cardoso**[1,2]
elaine.cardoso@unesp.br
[1]UNESP – São Paulo State University, Post-Graduation Program in Mechanical Engineering, Av. Brasil, 56, 15385-000, Ilha Solteira, SP, Brazil.
[2]UNESP - São Paulo State University, Campus of São João da Boa Vista, São João da Boa Vista, SP, Brazil

***Abstract:*** *Microchannel based heat sinks have proven to be an effective technique for cooling high energy density devices such as microprocessors. Two-phase systems provide high heat transfer coefficients for low mass fluxes values and a uniform surface temperature distribution. The present study experimentally evaluates the performance of a microchannel-based heat sink for convective boiling of HFE7100. The heat sink consists of 33 parallel rectangular channels of 10 mm in length, 200 μm in width, and 500 μm in height for each microchannel. Experimental data for heat transfer coefficient (HTC) and pressure drop are obtained under single-phase and two-phase flow conditions, for different mass fluxes values. It is observed an increase in HTC as the inlet subcooling and mass flux decrease; moreover, the pressure drop increases with an increase in mass flux and a decrease in the inlet subcooling. The correlations by Li and Wu (2010) and Kim and Mudawar (2012) are able to predict the two-phase HTC and pressure drop results with an absolute mean error of 16.14% and 79.37%, respectively.*

***Keywords:*** *HFE-7100, convective boiling, microchannels, pressure drop, heat transfer coefficient.*

## 1. INTRODUCTION

The size reduction of electronic devices leads to an increase in the dissipated heat flux. The use of microchannel-based heat exchangers (a commonly used name for channels with hydraulic diameters less than 3 mm) seems to be an alternative to keep the operating temperature of the device below its maximum temperature. According to Qu and Mudawa (2003) and Ribatski et al. (2007), a decrease in the channel diameter through which the fluid flows causes an increase in the surface contact area, which helps to reduce coolant inventory for the entire cooling system.

Due to the direct contact of the heated component with the working fluid, dielectric fluids such as fluorocarbons (FC-72, FC-87) and hydrofluoroethers (HFE7000, HFE7100, HFE7300) are considered a suitable choice for electronics cooling applications. These fluids have excellent qualities as low saturation temperatures (Leong, Ho, and Wong, 2017) and chemical properties compatible with the heated surface and other components. Additionally, HFE fluids present zero ozone depletion potential (ODP) and low global warming potential (GWP) (Misale, Guglielmini and Priarone, 2009).

Since the pioneering study on the microchannel heat sink by Tuckerman and Pease (1981), most of the micro heat exchangers have been designed by trial and error due to the lack of efficient prediction methods for the heat transfer coefficient. Most studies address different configurations of microchannels and working fluids, in order to understand the physical mechanisms responsible for the high HTC, the critical heat flux and the pressure drop. For example, Kim and Mudawar (2017) analyzed the convective boiling of HFE7100, R134a and water flowing in a multi-microchannel with the height ranged from 0.4 to 0.8 mm and width from 0.04 to 1 mm. The authors observed the behavior of the pressure drop, the average microchannel temperature and the critical heat flux for different operating conditions; as the width of the microchannels increased, the pressure drop decreased and the temperature of the heat exchanger increased. Dang et al. (2020) studied the HTC and the pressure drop behavior of HFE7000 convective boiling for different conditions in a multi-microchannel heat sink with 2 mm wide and 1 mm high; it was observed that an increase in the heat flux resulted in a pressure drop augmentation and a reduction in the pressure fluctuations at higher mass fluxes.

Al-Zaidi, Mahmoud and Karayiannis (2019) performed an analysis of HFE7100 convective boiling in a multi-microchannel heat sink (0.7 mm wide and 0.35 mm high) for five mass fluxes (ranging from 50 to 250 $kg/m^2s$). Flow

visualization and local heat transfer were obtained along the channels. The authors observed four flow patterns during the experiments: bubbly, slug, churn and annular flow. Moreover, the local two-phase heat transfer coefficient increased with a heat flux increase. Due to the rapid bubble generation near the channel inlet, flow reversal was observed for all mass fluxes; however, according to Al-Zaidi, Mahmoud and Karayiannis (2019), it did not affect the flow boiling heat transfer results.

In this context, we developed an experimental analysis on the performance of a heat sink based on muti-microchannels for convective boiling of HFE7100. Besides, we analyzed the pressure drop and surface temperature behavior as a function of the mass flux (392, 634 and 875 kg/m²s) and the inlet subcooling (5 and 10 ºC).

## 2. MATERIALS AND METHODS

### 2.1 Test Bench

The test section (Figure 1) consisted of a copper microchannel heat sink with 33 horizontal parallel rectangular microchannels. The copper block has overall dimensions of 10 mm in width ($W$) and 10 mm in length ($L$). The nominal dimensions of the microchannel (Figure 1 and Table 1) are 200 μm in width ($W_{ch}$), 500 μm in height ($H_{ch}$), and 100 μm channel wall thickness ($W_{th}$) for each microchannel. The tests were performed using HFE7100 as working fluid (saturation temperature equal to 61 °C at local atmospheric pressure, $p_{atm}$ = 98 kPa). A polycarbonate plate (2 mm thickness) covers the heat sink to allow flow visualization.

The microchannels were etched on a plain copper surface through micro-milling process by using CNC precision machining (located at Laboratory of Machines and Tools, LAMAFE - São Carlos School of Engineering - USP) with an uncertainty of ± 5 μm.

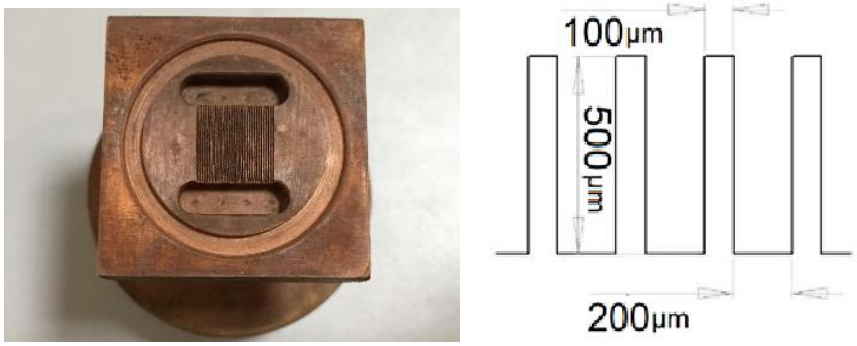


Figure 1. Microchannel heat sink scheme.

Table 1. Geometric parameters and dimensions of microchannels.

| | | | |
|---|---|---|---|
| **Heating perimeter (m)** | 0.0012 | **Footprint Area (m²)** | 0.0001 |
| **Number of microchannels [-]** | 33 | **Hydraulic diameter, $D_h$ (m)** | 0.000286 |
| **Length of microchannels, $L$ (m)** | 0.01 | **Microchannel width, $W_{ch}$ (m)** | 0.0002 |
| **Plenum surface area (m²)** | 0.00015 | **Microchannel Height, $H_{ch}$ (m)** | 0.0005 |

Figures 2 and 3 show an exploded view of the test section and a scheme of the experimental circuit, respectively. The working fluid was pumped from a liquid reservoir (Figure 3) to the flow loop; the HFE7100 flow rate was set by a rotameter (a pre-calibrated OMEGA model rotameter, with operating range from 10 to 500 ml/min) installed just upstream the pre-heater (consisted of a horizontal copper tube heated by an electrical tape resistance). There is a bypass line used for the test facility maintenance. The pressure drop between inlet and outlet plenums was measured by two pressure transducers (OMEGA PX309 model), assuming the pressure transducer uncertainty equal to that given by the manufacturer, 0.4 kPa. The flow temperature was measured using previously calibrated K-type thermocouples in the inlet and outlet plenums (both in contact with the fluid). The working fluid was cooled by a condenser and then returned to the reservoir.

Three K-type thermocouples were fixed within the heat sink wall to measure the wall temperature. The heat flux was generated by a cartridge-type electrical resistance (250 W/220 V), powered by a power source (Tectrol, Model TCA 300), into the bottom surface of the heat sink.

Figure 2. Test section assembly.

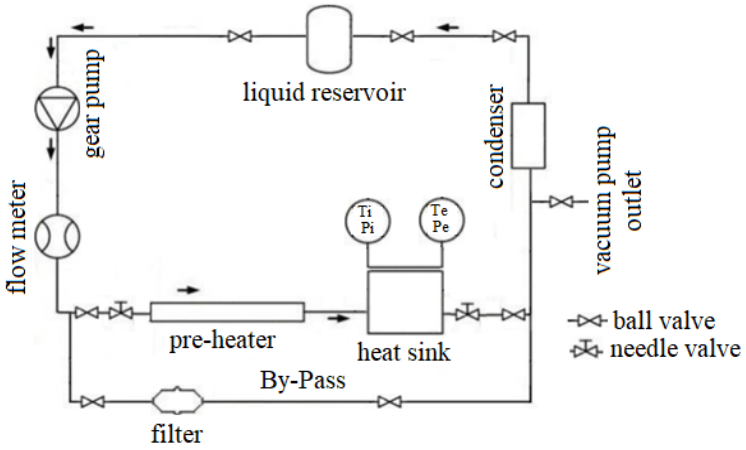


Figure 3. Schematic view of the experimental setup.

The thermal insulation of the entire test section (Figure 2) was made with polytetrafluoroethylene. The acquisition of the temperature and pressure values was performed by an Agilent data acquisition system 34970A.

### 2.2 Experimental Procedure

The validation aims to verify the coherence of the results obtained experimentally; thus, it was performed in a single-phase regime in order to compare the experimental results with well-established correlations from literature. Moreover, numerical analysis for the single-phase flow of HFE7100 was carried out and compared with experimental data and analytical results obtained from correlations found in the literature.

The mass, momentum and energy conservation equations with the second-order upwind schemes, and the flow steady-state, incompressible and laminar, were solved adopting the Finite-Volume Method implemented in ANSYS Fluent V15; the SST κ-ω model was used for modeling the turbulence. As a reference pressure, atmospheric pressure was defined; by considering the characteristics of a low-pressure system, the outlet pressure was set up as zero. No-slip condition was considered on the surfaces. Inlet velocity was calculated as a function of the microchannels number, mass flux (from the experimental approach), and dimensions of the microchannel cross-section. The heat flux was distributed through the microchannel sides except for the top side (the heat sink was thermally insulated by a polycarbonate piece, Figure 2); for the inlet and outlet plenums, adiabatic wall conditions were considered.

The convergence occurred for meshes with 99873 elements; the finer mesh was achieved when residuals were less than $10^{-5}$ for continuity equation and $10^{-6}$ for momentum and energy equations. The simulations used the segregated algorithm with SIMPLE algorithm for pressure-velocity coupling.

After the validation, two-phase flow tests were performed for two different subcooling values, 5 ºC and 10 ºC; mass fluxes of 392, 634 and 875 kg/m²s; and, for different footprint heat fluxes from 55 to 677 kW/m². The fluid flow rate was set by adjusting the pump speed and rotameter, the preheater was adjusted until its outlet temperature was equal to the desired subcooling, of 5 °C or 10 °C. A data acquisition system (Agilent 34970A) recorded the data every 10 seconds after the system attained a steady-state regime. The same procedure was adopted for all experimental tests.

## 3. METHODOLOGY

The footprint area-based heat flux ($q^{"}_{footprint}$) is given by,

$$q^{"}_{footprint} = \frac{\dot{Q}}{A_{footprint}} \tag{1}$$

where the effective power ($\dot{Q}$) is equal to the total heat rate supplied to the microchannel heat sink, corresponding to the electrical power subtracted from the heat losses (to the environment and also to the fluid at the inlet and outlet plenums, $\dot{Q_{loss}}$). It is worth mentioning that all analyses take into account the real heat flux (the heat flux dissipated through the microchannels).

The footprint heat transfer coefficient is given by Newton's cooling law, as shown in equations (2) and (3):

$$\overline{h_{footprint}} = \frac{q"_{footprint}}{\Delta T} \tag{2}$$

$$\Delta T = \overline{T_W} - \overline{T_f} \tag{3}$$

where $\overline{T_W}$ is the average temperature of the microchannels given by three K-type thermocouples fixed within the heat sink wall, and the average temperature of the fluid ($\overline{T_f}$) is given by the same procedure as Leão, Nascimento and Ribastki (2014).

Pressure transducers (at inlet and outlet plenums, $P_i$ and $P_e$, respectively) were utilized to measure the pressure drop in the region between the inlet and outlet plenums; and the pressure drop through the microchannels ($\Delta P_{microchannel}$) [Pa] is given as follows:

$$\Delta P_{measured} = P_i - P_e \tag{4}$$

$$\Delta P_{microchannel} = \Delta P_{measured} - \Delta P_{contraction} - \Delta P_{expansion} \tag{5}$$

where the pressure drops due to contraction and expansion ($\Delta P_{contraction}$ and $\Delta P_{expansion}$, respectively) are obtained by the method described in Chalfi and Ghiaasiaan (2008).

### 3.1 Uncertainty Analysis

The uncertainty relating to the geometric parameters of the heat sink, such as height (H), width (W) and length (L) of the microchannel is given from its manufacturing process. For the power supply voltage and the resistance, the uncertainty is obtained from the uncertainty of measurement instruments. The pressure transducer uncertainty is assumed to equal to that given by the manufacturer. To calculate the remaining uncertainties, the Abernethy and Thompson (1983) method and the Kline and McClintock method (described in Figliola and Beasley (2006)) are used. Table 2 presents the uncertainties for all dimensional parameters.

Table 2. Uncertainty of dimensional parameters.

| Parameter | Uncertainty | Parameter | Uncertainty | Parameter | Uncertainty |
|---|---|---|---|---|---|
| $H$ [mm] | 0.005 | $P$ [kPa] | 0.4 | $q''_{footprint}$ [kW/m²] | 1% a 6% |
| $W$ [mm] | 0.005 | $T$ [ºC] | 0.3 | $G$ [kg/m²s] | 2% a 6% |
| $L$ [mm] | 0.005 | Flow rate [ml/min] | 2.77 | $h_{footprint}$ [kW/m²K] | 2% a 8% |
| Voltage [V] | 0.1 | Resistance [Ω] | 1 | $\Delta P$ [kPa] | 0.5 |
| | | | | $\Delta T$ [ºC] | 0.4 |

## 4. RESULTS AND DISCUSSION

### 4.1 Consistency Analysis

For consistency analysis of the apparatus and the experimental procedure, single-phase validation was first carried out before conducting two-phase flow tests. Figure 4a shows the numerically and experimentally determined pressure drop for different mass fluxes compared with the correlations given by Shah and London (1978), which were proposed for laminar developing and fully developed flow in horizontal non-circular channels.

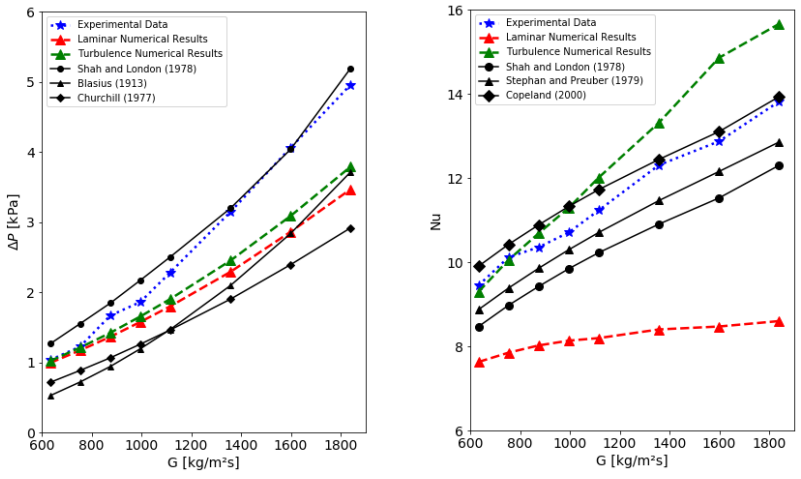


(a) (b)

Figure 4. Consistency analysis for a footprint area-based heat flux of 60 kW/m². (a) Pressure drop and (b) Nusselt number.

There was a good agreement between the experimental results and the correlation for fully developed flow with a mean absolute error ($MAE = \frac{1}{N}\sum_1^N \frac{|\phi_{exp}-\phi_{pred}|}{\phi_{exp}} \times 100\%$ ) of 11.6%; the same behavior was found for both laminar and turbulent numerical simulation with MAE of 18.7% and 14.4%, respectively.

The average Nusselt number *versus* mass flux was compared with numerical simulation and three existing correlations Shah and London (1978), Stephan and Preuber (1979) and Copeland (2000) as shown in (Figure 4b). The experimental data were predicted well by the turbulent numerical simulation (MAE = 6.9%); this good performance comes from the appearance of a turbulent viscosity when the turbulent modeling is implemented, which leads to a better agreement of the computational results with the experimental results, being an indication that turbulence may arise, even for the Reynolds number range considered. The single-phase results described demonstrate that the measurement system and calibration can provide accurate results for the flow boiling experiments.

### 4.2 Boiling Curves

Figures 5a and 5b show the effect of different inlet subcooling temperatures (5 and 10 °C) and different mass fluxes (392, 634 and 875 kg/m²s) on the boiling curves of HFE7100, respectively. An increase in the subcooling shift the boiling curve to the right, a behavior similar to that found by Leão, Nascimento and Ribatski (2014); according to them, this is due to the lower fluid temperature at the microchannel inlet, which causes a decrease in the portion of the microchannels under the effects of convective boiling. Thus, there is a larger region of the channels under forced convection effects in which the heat transfer coefficient is lower compared to the convective boiling.

For high heat fluxes, the curves for the same mass flux are consistent with the results obtained by Park and Thome (2010). The portion of the fluid in the single-phase flow presented in the heat sink tends to be smaller and this effect becomes more pronounced at lower mass fluxes, i.e., the single-phase region becomes negligible compared to the two-phase flow length and no influence of inlet subcooling temperature is observed. Moreover, a negligible temperature overshoot is observed (in the present work, the temperature overshoot was only observed for mass fluxes of 392 kg/m$^2$ s). As mentioned by Park and Thome (2010), a high-pressure drop at high mass flux conditions favors the flashing effect, which had advantages to reduce the wall-temperature overshoot at the onset of boiling.

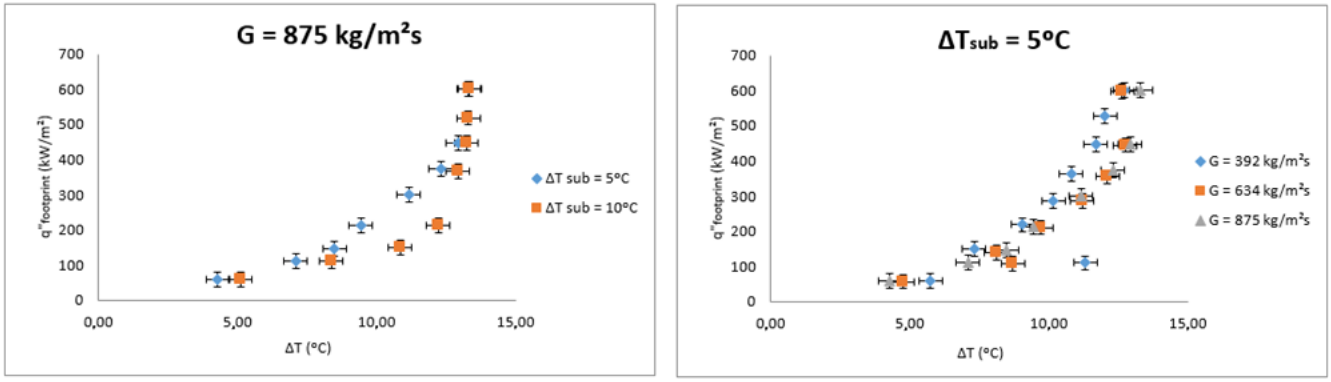


(a) (b)

Figure 5. Boiling curve for HFE7100. (a) Effect of inlet subcooling temperatures for $G$ = 875 kg/m$^2$s and (b) Mass flux effect for $\Delta T_{sub}$ = 5 ºC.

The behavior presented in Figure 5b can also be explained by the portion of the heat sink under the effect of convective boiling. As the mass flux increases the heat supply needed to initiate bubble nucleation also increases, i.e., for the same heat flux value, the single-phase region is larger reducing the HTC and, consequently, shifting the boiling curve to the right. At high heat fluxes, according to Harirchian and Garimella (2008), convective boiling is predominant and the influence of mass flux on the boiling curve becomes negligible (Figure 5b and $q''_{footprint}$ > 500 kW/m$^2$).

### 4.3 Heat Transfer Coefficient

In the single-phase region and at the same mass flux, the HTC values are constant regardless of inlet subcooling and footprint area-based heat flux (Figure 6a). At the point where the onset of nucleate boiling occurs the HTC sharply increases and the curve is characterized by an almost linear variation of the HTC with the heat flux, as also found by Dent et al. (2015).

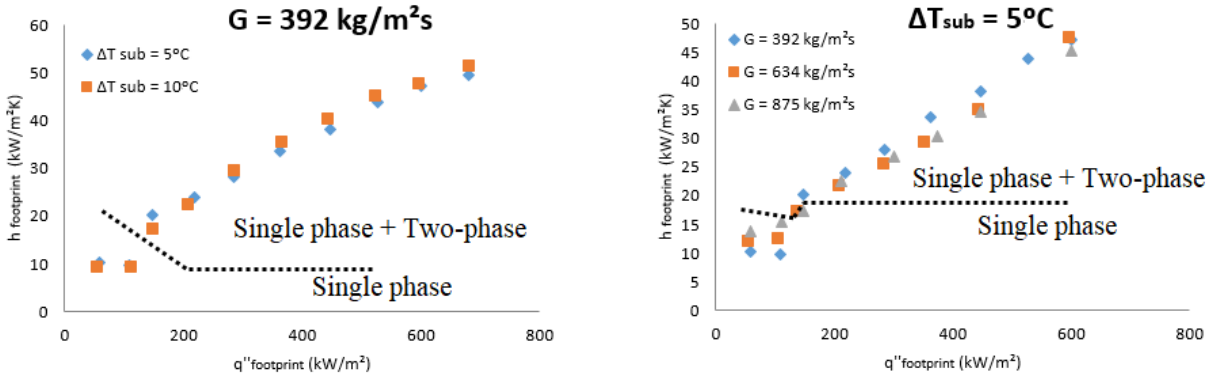


Figure 6. HTC curve. (a) Effect of inlet subcooling temperatures for $G$ = 392 kg/m$^2$s and (b) Mass flux effect for $\Delta T_{sub}$ = 5 ºC.

Figure 6b shows the effect of wall heat and mass fluxes on the HTC for an inlet subcooling of 5 ºC; the experimental results indicate an insignificant mass flux effect with a strong heat flux effect on HTC.

### 4.4 Pressure Drop Curves

Figures 7a and 7b show the variation of the total pressure drop with base heat flux for different inlet subcooling and mass fluxes, respectively. In the two-phase flow region, the pressure drop increases rapidly with the heat flux as the rate of vapor generation becomes pronounced. Moreover, as the inlet subcooling decreases the pressure drop becomes larger, at the same heat flux value (a lower inlet subcooling temperature of the fluid results in a higher vapor quality along the microchannels, leading to a larger pressure drop as also observed by Sempértegui-Tapia and Ribatski, 2017).

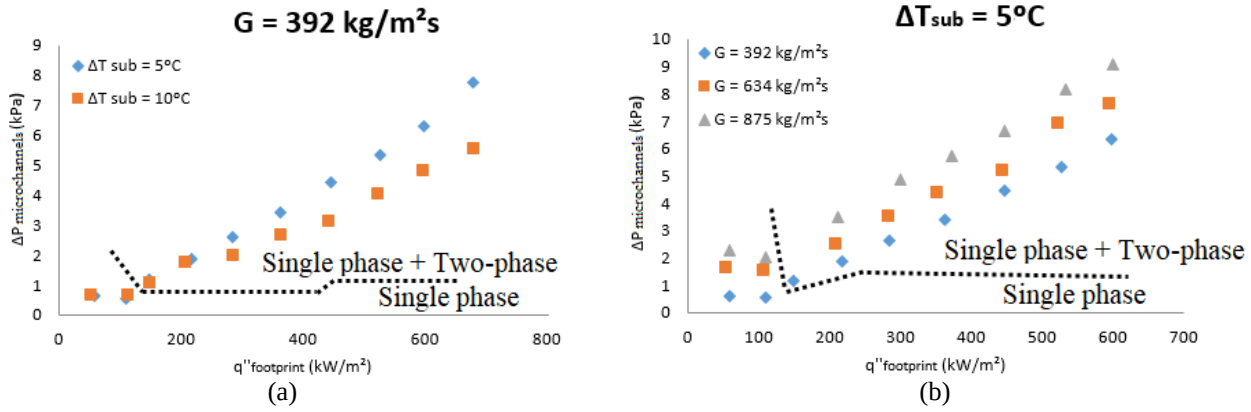


Figure 7. Pressure drop curve. (a) Effect of inlet subcooling temperatures for $G$ = 392 kg/m$^2$s and (b) Mass flux effect for $\Delta T_{sub}$ = 5 ºC.

Figure 7b shows that the pressure drop increases with increasing heat flux and with increasing mass flux.

### 4.5 Evaluation of Heat Transfer Correlations

The results obtained experimentally for HTC were compared with the well-known correlations from the literature. Five existing two-phase heat transfer correlations were selected and compared with the experimental results for the two-phase flow region (Table 3).

Table 3. Comparison between the experimental data and the flow boiling predictive correlations.

| Correlation | Mean Absolute Error (MAE) | Percentage predicted within ±30% of data |
|---|---|---|
| Li and Wu (2010) | 16.1 % | 90.9 % |
| Kim and Mudawar (2013) | 17.3 % | 84.1 % |
| Liu and Winterton (1991) | 34.6 % | 36.4 % |
| Mahmoud and Karayiannis (2013) | 42.6 % | 2.3 % |
| Chen (1966) | 71.2 % | 0.0 % |

The correlations of Li and Wu (2010) and Kim and Mudawar (2013) predicted the data very well, predicting 90.9% and 84.1% of the data within the ±30% error band and with mean absolute error (MAE) of 16.1% and 17.3%, respectively. These correlations were developed based on an extensive database (4228 and 10805 data, respectively) for different working fluids.

The Liu and Winterton (1991) correlation predicted correctly 36.4% of the database. This correlation includes micro and mini-channel data with hydraulic diameters ranging from 2.95 to 32 mm (values much larger than the hydraulic diameter used in the present study, $D_h$ = 0.28 mm). Mahmoud and Karayiannis (2013) proposed an empirical correlation for flow boiling of R134a in vertical stainless steel microtubes ranging from 0.52 to 4.26 mm. This correlation predicted only 2.3% of the data within the ±30% error band with a MAE of 42.6%.

### 4.6 Evaluation of Pressure Drop Correlations

The experimental flow boiling pressure drop data were compared to different two-phase pressure drop correlations available in the literature (Table 4).

Table 4. MAE and the percentage predicted data within ± 30% error bands for flow boiling pressure drop correlations.

| Correlation | Mean Absolute Error (MAE) | Percentage predicted within ±30% of data |
|---|---|---|
| Li and Wu (2010) | 117.7 % | 33.3 % |
| Zhang, Hibiki and Mishima (2010) | 76.5 % | 58.3 % |
| Cicchitti et al. (1960) | 84.9 % | 4.1 % |
| Müller-Steinhagen and Heck (1986) | 70.7 % | 4.1 % |
| Sempertegui-Tapia and Ribatski (2017) | 334.8 % | 8.3 % |
| Kim and Mudawar (2012) | 79.3 % | 58.3 % |
| Lockhart and Martinelli (1949) | 133.1 % | 16.6 % |

According to Table 4, the best two predictive methods were Kim and Mudawar (2012) and Zhang, Hibiki and Mishima (2010), both predicting 58.3% of the experimental data within the ± 30% error band.

The correlations of Sempertegui-Tapia and Ribatski (2017), Lockhart and Martinelli (1949) and Müller-Steinhagen and Heck (1986) predicted only 8.3%, 16.6% and 4.1% of experimental data within ± 30% error bands. The poor predictability of these correlations may be related to the effects of flow reversal and boiling instability, very common in multi-microchannel configurations.

Li and Wu (2010) correlation reasonably predicted the experimental data with 33.3% in the ± 30% error bands. The performance of the Cicchitti et al. (1960) correlation may be due to the liquid and vapor phases being treated as one homogenous phase flow, i.e., both phases are modeled as one continuous phase and the slip velocity between the phases is assumed to be negligible.

## 5. CONCLUSIONS

In this experimental study, single-phase and flow boiling heat transfer and pressure drop were investigated in a multi-microchannels heat sink with a hydraulic diameter of 0.28 mm using HFE-7100 as the working fluid.

The tests were performed with three different mass fluxes (392, 634 and 875 kg/m²s) and two inlet subcooling temperatures (5 and 10 ºC). The key findings that can be drawn from this study are:

- ✓ The consistency analysis showed satisfactory results, with experimentally values for pressure drop and the Nusselt number close to those predicted by well-established correlations from literature. Moreover, numerical analysis for the single-phase flow of HFE7100 was carried out, showing good agreement with the experimental results.
- ✓ An increase in the subcooling shift the boiling curve to the right, due to the lower fluid temperature at the microchannel inlet leads to a larger region of the channels under forced convection effects in which the heat transfer coefficient is lower as compared to the convective boiling.
- ✓ A negligible temperature overshoot is observed for mass fluxes higher than 392 kg/m$^2$s. A high-pressure drop at high mass flux conditions favors the flashing effect, which had advantages to reduce the wall-temperature overshoot at the onset of boiling.
- ✓ As the mass flux increases the heat supply needed to initiate bubble nucleation also increases, and consequently, the boiling curve is shifted to the right. At high heat fluxes, the influence of mass flux on the boiling curve becomes negligible.
- ✓ At the onset of nucleate boiling the HTC sharply increases and the curve is characterized by an almost linear variation of the HTC with the heat flux; moreover, it is observed an insignificant mass flux effect with a strong heat flux effect on HTC.

- ✓ In the two-phase flow region, the pressure drop increases rapidly as heat flux and mass flux increase regardless of the inlet subcooling temperature.
- ✓ The correlations proposed by Li and Wu (2010) and Kim and Mudawar (2013) predicted the experimental data very well, with 90.9% and 84.1% of the data within the ±30% error band.
- ✓ The flow boiling pressure drop correlations of Kim and Mudawar (2012) and Zhang, Hibiki and Mishima (2010) reasonably predicted the experimental flow boiling pressure drop results, with 58.33% of the values in the ± 30% error bands.

## 6. ACKNOWLEDGEMENTS

The authors are grateful for the financial support from the PPGEM – UNESP/FEIS, from the National Council of Technological and Scientific Development of Brazil (CNPq grant number 458702/2014-5) and FAPESP (grants numbers 2013/15431-7 and 2019/02566-8).

## 7. REFERENCES

Abernethy, R.B. and Thompson, J.W., 1983. *Handbook, Uncertainty in gas turbine measurement.* National Technical Information Service, Springfield.

Al-Zaidi, A.H., Mahmoud, M.M. and Karayiannis, T.G., 2019. "Flow boiling of HFE-7100 in microchannels: Experimental study and comparison with correlations". *International Journal of Heat and Mass Transfer,* Vol. 140, pp.100-128.

Blasius, H., 1913. "Das Aehnlichkeitsgesetz bei Reibungsvorgängen in Flüssigkeiten". *Mitteilungen über Forschungsarbeiten auf dem Gebiete des Ingenieurwesens,* Vol. 131, pp. 1-41.

Chalfi, T.Y. and Ghiaasiaan, S., 2008." Pressure drop caused by flow area changes in capillaries under low flow conditions". *International Journal of Multiphase Flow,* Vol. 34, No. 1, pp. 2 – 12.

Chen, J.C., 1966. "Correlation for boiling heat transfer to saturated fluids in convective flow". *I&EC process design and development,* Vol. 5, pp. 323–329.

Churchill, S.W., 1977. "Friction-factor equation spans all fluid-flow regimes". *University of Pennsylvania,* Vol 87, No. 24, pp. 91-92.

Cicchitti, A., Lombardi, C., Silvestri, M., Soldaini, G. and Zavat-Tarelli, R., 1960. "Two-phase cooling experiments-pressure drop, heat transfer and burnout measurements". *Energia Nucleare,* Vol. 7, pp. 407–425.

Copeland, D., 2000. "Optimization of parallel plate heatsinks for forced convection". In *Six-Teenth Annual Ieee Semiconductor Thermal Measurement and Management Symposium - Semi-Therm 2000.* San Jose, USA.

Dang, C., Jia, L., Peng, Q., Yin, L. and Qi, Z., 2020. "Comparative study of flow boiling heat transfer and pressure drop of HFE-7000 in continuous and segmented microchannels". *International Journal of Heat and Mass Transfer,* Vol. 148, pp. 119038.

Deng, D., Wan, W., Tang, Y., Wan, Z. and Liang, D. 2015. "Experimental investigations on flow boiling performance of reentrant and rectangular microchannels- a comparative study". *International Journal of Heat and Mass Transfer,* Vol. 82, pp. 435 – 446.

Figliola, R.S. and Beasley, D.E., 2006. *Theory and Design for Mechanical Measurements.* John Wiley & Sons, New Jersey, 4th edition.

Harirchian, T. and Garimella, S. V., 2008. "Microchannel size effects on local flow boiling heat transfer to a dielectric fluid". *International Journal of Heat and Mass Transfer,* Vol. 51, No. 15-16, pp. 3724 – 3735.

Kim, S.M. and Mudawar, I., 2012. "Universal approach to predicting two-phase frictional pressure drop for adiabatic and condensing mini/micro-channel flows". *International Journal of Heat and Mass Transfer,* Vol. 55, No. 11-12, pp. 3246 – 3261.

Kim, S.M. and Mudawar, I., 2013." Universal approach to predicting saturated flow boiling heat transfer in mini/micro-channels – Part I. Dryout incipience quality". *Int. J. Heat Mass Transfer,* Vol. 64, pp. 1229-1238.

Kim, S.M. and Mudawar, I., 2017. "Thermal design and operational limits of two-phase microchannel heat sinks". *International Journal Of Heat And Mass Transfer,* Vol. 106, pp.861-876.

Leão, H.L.S.L., Nascimento, F.J. and Ribatski, G., 2014. "Flow boiling heat transfer of r407c in a microchannels based heat spreader". *Experimental Thermal and Fluid Science,* Vol. 59, pp. 140 – 151.

Leong, K.C., Ho, J.Y. and Wong, K.K., 2017. "A critical review of pool and flow boiling heat transfer of dielectric fluids on enhanced surfaces". *Applied Thermal Engineering*, Vol. 112, pp. 999-1019.

Li, W. and Wu, Z., 2010. "A general correlation for evaporative heat transfer in micro/ mini-channels". *Int. J. Heat Mass Transfer,* Vol. 53, pp. 1778–1787.

Liu, Z. and Winterton, H.S., 1991. "A general correlation for saturated and subcooled flow boiling in tubes and annuli, based on a nucleate pool boiling equation". *International Journal of Heat and Mass Transfer*, Vol. 34, pp.2759–2766.

Lockhart, R.C. and Martinelli, R.C. 1949. "Proposed correlation of data for isothermal two-phase two-component flow in pipes". *Chemical Engineering Progress*, Vol. 45, pp. 39–48.

Misale, M., Guglielmini, G. and Priarone, A., 2009. "HFE-7100 pool boiling heat transfer and critical heat flux in inclined narrow spaces". *International Journal of Refrigeration*, Vol. 32, No. 2, pp.235-245.

Mahmoud, M.M. and Karayiannis, T.G., 2013. "Heat transfer correlation for flow boiling in small to microtubes". *Int. J. Heat Mass Transf,* Vol. 66, pp. 553–574.

Müller-Steinhagen, H. and Heck, K., 1986. "A simple friction pressure drop correlation for two-phase flow in pipes". *Chemical Engineering and Processing: Process Intensification,* Vol. 20, pp. 297–308.

Park, E.J. and Thome, J.R., 2010. "Critical heat flux in multi-microchannel copper elements with low-pressure refrigerants". *International Journal of Heat and Mass Transfer*, Vol. 53, No. 1-3, pp. 110-122.

Qu, W. and Mudawar, I., 2003. "Measurement and prediction of pressure drop in two-phase microchannel heat sinks". *International Journal of Heat and Mass Transfer*, Vol. 46, pp. 2737-2753.

Ribatski, G., Zhang, W., Consolini, L., Xu, J. and Thome, J.R., 2007. "On the Prediction of Heat Transfer in Micro-Scale Flow Boiling". *Heat Transfer Engineering,* Vol. 28, No. 10, pp.842-851.

Sempértegui-Tapia, D, F and Ribatski, G., 2017. "Two-phase frictional pressure drop in horizontal micro-scale channels: experimental data analysis and prediction method development". *International Journal of Refrigeration*, Vol. 79, pp. 143-163.

Shah, R. K., London, A. L., 1978. "Rectangular Ducts. Laminar flow forced convection in ducts". *Academic Press,* pp. 196-222.

Stephan, K., Preuber, P., 1979. "Wärmeübergang und maximale wärmstromichte beim behältersieden binärer und ternärer flüssigkeitsgemische". *Cheime Ingenieur Technik*, Vol. 51, No. 1, pp. 37-37.

Tuckerman, D.B. and Pease, R.F.W., 1981. "High-performance heat sinking for VLSI". *IEEE Electron Device Letters,* Vol. 2, No. 5, pp. 126-129.

Zhang, W., Hibiki, T. and Mishima, K., 2010. "Correlations of two-phase frictional pressure drop and void fraction in minichannel". *Int. J. Heat Mass Transfer,* Vol. 53, pp. 453–465.

## 8. RESPONSIBILITY NOTICE

The authors are the only responsible for the printed material included in this paper.